

On Self-cleaning and Anti-ice Performance of Double-layer SAMs Coatings with Enhanced Corrosion Resistance on an Al Alloy Substrate

S. Farhadi¹, M. Farzaneh¹ and S. Simard²

¹Canada Research Chair on Atmospheric Icing Engineering of Power Networks (INGIVRE), Université du Québec à Chicoutimi, QC, Canada

²Aluminum Technology Centre, Industrial Materials Institute, National Research Council Canada (CNRC) 501, boul. de l'Université Est, Chicoutimi, QC, Canada

Email: shahram.farhadi@uqac.ca

Abstract: In cold climate regions, outdoor structures including transmission lines and telecommunication networks are exposed to ice and/or snow accretions which may result in damage and malfunctions. Superhydrophobic coatings were introduced and developed over the past decades as a passive technique to reduce or prevent ice accumulation on outdoor structures. At the same time, corrosion protection of metallic substrates such as aluminium and its alloys is another important issue when they are used in environments in close contact with water or other aggressive molecules. The present study, therefore, aims at systematically studying a double-layer SAMs coating terminated with surface alkyl groups that are expected to reduce ice adhesion and corrosion rates on an Al surface. More precisely, thin films of 1,2-bis-trioxyethyl-silyl-ethane [$C_{14}H_{34}O_6Si_2$] and octadecyltrimethoxysilane [$C_{18}H_{37}Si(OCH_3)_3$] were deposited layer by layer on etched Al alloy (AA2024-T3) substrates. The first layer was used as an underlayer expecting to improve the anti-corrosive performance for the top-layer providing surface water and ice repellency (surface hydrophobization). The prepared coated samples demonstrated good superhydrophobic and self-cleaning properties providing a static water contact angle of $CA > 155^\circ$ and a hysteresis angle of $CAH \leq 5^\circ$. The low CAH causes the water droplets to roll off the surface easily carrying away surface contamination by water droplets passing by. The coating stability was studied by immersing the coated samples into water, with basic and acidic conditions (different pH), showing gradual loss of superhydrophobicity over time. In the meantime, while bare mirror-polished and as-received Al showed average ice detachment shear stress values of $\sim 270 \pm 20$ kPa and $\sim 370 \pm 30$ kPa, respectively, their counterparts coated samples showed reduced values of $\sim 182 \pm 15$ kPa. This reduction is ascribed to the presence of engineered micro-/nano-hierarchical surface asperities along with the applied low surface energy top-layer on the sample surface. The ice-releasing performance, however, gradually decreased over repeated icing/de-icing cycles. Potentiodynamic polarization studies revealed that the corrosion resistance of modified aluminium alloy improved remarkably compared to the unmodified samples. Meanwhile, cyclic corrosion exposure tests demonstrated that while extensive corrosion appeared on bare Al after only 8 cycles of salt spray exposure, trace of corrosion was observed for the double-layer SAMs coating after 81 cycles of exposure.

Keywords: *superhydrophobicity; self-cleaning; anti-corrosive performance; nanostructured aluminum; double-layer coating; durability; ice repellency; wetting hysteresis.*

INTRODUCTION

Atmospheric icing occurs when the surface of exposed structures comes into contact with supercooled water droplets or snow particles. Ice and wet snow accumulation and adhesion on outdoor structures or equipment are well known to be a serious issue in cold climate countries [1]. In the specific case of power transmission lines, ice/wet snow may cause serious damage due to their high adherence to both metallic and insulator surfaces [1]. Each year, numerous failures due to ice accumulation are reported in Canada, USA, Iceland, Japan and so forth. Prevention of icing requires reducing its adhesive strength. Therefore, a variety of de-icing and anti-icing techniques were developed over the last decades [2]. Most of the efforts in recent years have been devoted to develop more efficient systems to prevent icing. While most of the techniques currently in use are active de-icing methods, e.g. thermal, electrical, chemical or mechanical techniques, all are used where accumulations are considerable and therefore, they consume a great deal of energy. Passive approaches, e.g. development of anti-icing or icephobic coatings that inhibit ice accumulation, are gaining in popularity [2, 3, 4]. Alkyl-terminated coatings, e.g. alkylsilane-based layers, were previously proposed as potentially ice-releasing coatings [4, 5, 6]. Reasonable correlation between hydrophobicity and ice repellency has been reported earlier [3, 6-8]. Superhydrophobic surfaces defined as surfaces with static water contact

angle larger than 150° and low hysteresis, $CA_H < 6$, have attracted considerable interest in this area. It is well known that the key factors underlying superhydrophobicity is the chemical composition of the surface along with a micro-/nano-hierarchical texture [3, 5, 6, 9]. Superhydrophobicity can also improve self-cleaning and anti-corrosive properties of Al alloys [4, 10-12] as it can prevent penetration of water molecules or other aggressive moieties into the metallic surface underneath [11, 12]. Arianpour *et al.* [9] reported delayed water freezing on rough superhydrophobic surfaces. In the meantime, metal corrosion should also be taken into account since metal or metallic alloys are subject to corrosion problems when exposed to aggressive environments. For this reason, in the development of anti-ice coatings on Al surface, they must not only be durable enough, but also provide anti-corrosive protection of that specific metal. It would be interesting for industrial applications to introduce new coatings which would be more specifically environmentally friendly alternatives to the currently used toxic chromate-based coatings and which would be anticorrosive.

In the present study, organic coatings terminated with alkyl groups were prepared as potential ice/snow-repellent layers on the surface of etched aluminium alloy 2024 (AA2024) for one-layer and multilayer approaches. More precisely, a thin film of octadecyltrimethoxysilane [ODTMS] as top-layer (water repellent coating) on an underlayer of 1,2-bis-trioxymethyl-silyl-ethane [BTSE] (providing a high density of -OH groups on the surface for the top-layer of ODTMS), were applied on Al substrates. These nanostructured surfaces were characterized and their coating stability (in water, basic and acidic conditions) and ice-repellent performance were carefully studied. To study their anti-corrosive performance, potentiodynamic polarization tests as well as cyclic corrosion exposure tests were carried out.

I. EXPERIMENTAL PROCEDURE

A. Sample Preparation

The AA2024-T3 panels from industrial rolled sheets were cut into smaller plates with dimensions of 2×2 and 5.1×3.2 cm² and were used as substrates. This Al alloy, whose Cu content as the primary alloying element is typically between 3.8-4.9 % (wt. %) [13, 14], is used extensively in applications that require high strength to weight ratio as well as good fatigue resistance. The as-received Al substrates, 2-mm thick, were ultrasonically cleaned and degreased in water and organic solvents (acetone and absolute ethanol), each for 5 min. The unpolished cleaned samples were then etched in ~9 wt % HCl at room temperature for 3 min. This was followed by ultrasonically rinsing 2-3 times in deionized water to remove any unstable particles on the surface resulting from the etching process. The etched samples were dried in a N₂ flow and were kept in oven at 80°C for 3 hrs. The pre-treated samples were then placed in baths with different chemicals at room temperature. The deposition baths for the top layer was ODTMS 1% (V/V%) from SIGMA-ALDRICH® in isopropanol (ACS grade with water content of <0.2%)-deionized water, as solvent. Prior to use, the bath were vigorously stirred for 3 hrs to allow for dissolution/hydrolysis. A BTSE solution (4.7 ml in isopropanol-water) for silane deposition was prepared to deposit the underlayer. These conditions could offer the best compromise between silane hydrolysis and condensation [15]. Rough Al samples were dipped into the BTSE solution for 1 min followed by blow-drying in N₂ and were then immersed into the ODTMS-isopropanol bath solution for 15 min. Upon coating and prior to tests, the modified samples were removed from their corresponding solutions, rinsed with copious amounts of isopropanol and blown-dried with N₂. They were then annealed in ambient atmosphere at 80 °C for 5hrs to remove any volatile components or residual solvents and to improve coating cross-linking [16]. Sample characterizations were done immediately following sample preparation. While the smaller samples were used to test stability of the coatings in various conditions, the larger ones were further used to evaluate their ice-repellent and anti-corrosive performance.

B. Sample characterization

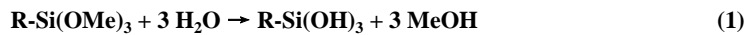
The sample stability in water, basic and acidic conditions was studied by means of CA measurements on samples immersed in nanopure water, tap water as well as basic (pH: 10.1) and acidic (pH:4) buffer solutions at ~18-20 °C. The wetting characteristics, reported in Fig. 2, were obtained following the standard sessile drop method on a DSA100 goniometer from Krüss [4, 6, 16]. For each sample, at least three different spots were randomly measured and the CA reported was the average value of about 5 measurements. Surface topographies were studied by means of scanning electron microscopy (SEM, Hitachi FEGSEM-SU 70) in high-vacuum mode. X-ray photoelectron spectroscopy (XPS) was performed with a Quantum-2000 instrument from PHI and an X-Ray source of achromatic Al K α . (1486.6 eV). The ice adhesion test was conducted by creating glaze ice (up to ~1 cm thick and ~4-5 gr weight) over $\sim 3.2 \times 3.0$ cm² surface

area and prepared by spraying supercooled micro-droplets of water (average size of $\sim 65 \mu\text{m}$) in a wind tunnel at subzero temperature (-10°C), wind speed of 11 ms^{-1} , water pressure of 325 kPa , and water feed rate of 6.3 gm^{-3} . The iced samples were then spun in the centrifuge at constantly increasing speed. Potentiodynamic polarization was used to examine the overall corrosion behaviour of the bare and coated Al samples. The working cell was a standard three-electrode cell with working electrode area of 1 cm^2 . A platinized net and saturated calomel electrode (SCE) were used as counter and reference electrodes, respectively. The setup used to control the experiments was a potentiostat system composed of a Solartron SI1287A electrochemical interface (controlled by Corrware[®] software). Measurements were performed in 3.5 wt.% NaCl solutions at room temperature. Potentiodynamic polarization curves were established and the corrosion potential (E_{corr}) and corrosion current density (i_{corr}) were determined using the *Tafel* extrapolation method. The polarization scan was started from 250 mV below the open circuit potential (OCP) in the cathodic region, through the corrosion potential, and 250 mV above the open circuit potential in the anodic region and with a constant scan rate of 1 mVs^{-1} . Finally, the Al panels were placed into a cyclic corrosion test chamber (*Ascott*) with the unmodified surface protected by a scotch tape and the the modified surfaces exposed alternatively to salt mist, dry and wet conditions in accordance with ISO14993-Corrosion of Metals and Alloys [17].

II. RESULTS AND DISCUSSION

A. Coating durability in different pH condition

The aluminium alloy is a hydrophilic material with a native oxidized thin layer ($\sim 4 \text{ nm}$ thickness) demonstrating water CA and surface energy of $\sim 41.5 \pm 3^\circ$ and $46.36 \pm 1.64 \text{ (mNm}^{-1}\text{)}$, respectively. The Al substrates were etched in diluted HCl for 3 minutes followed by immersion in a BTSE or ODTMS solution. By immersing the Al samples in HCl, they react with HCl and AlCl_3 is produced while $\text{H}_2\uparrow$ is released. Bare etched Al showed water CA and surface energy of $\sim 21.2 \pm 5^\circ$ and $68.30 \pm 1.16 \text{ (mNm}^{-1}\text{)}$, respectively. Prior to deposition, the baths were vigorously stirred for 3 h to allow adequate dissolution/hydrolysis according to the following reaction:



The freshly formed thin layer of metal oxide on the Al surface reacted with precursor molecules (BTSE) to form a covalently bound coating on the Al substrate. The CA value at this step was measured after the BTSE deposition was $\sim 41^\circ$. After ODTMS deposition, however, the double layer coating (BTSE/ODTMS) demonstrated initial values of $\text{CA} > 150^\circ$ (Figures 2 and 3a) and $\text{CAH} < 6^\circ$ indicating the presence of well-coated rough Al surfaces. The CA measured on a flat Al sample coated with ODTMS alone is $\sim 111 \pm 2^\circ$. However, if the sample is etched for 5 min, it shows hydrophobic properties as its CA and CAH values are $\sim 143.4^\circ \pm 2$ and $\sim 12.1^\circ$, respectively. These CA and CAH values imply that water droplets rest at the top of rough asperities on the solid-air composite surface (Cassie-Baxter wetting regime). In this regime, CA can be expressed as follows:

$$\mathbf{\text{Cos}\theta^* = f (1 + \text{Cos}\theta) - 1} \quad (2)$$

where θ^* and θ are the CA of rough and flat surfaces with the same surface chemistry, respectively, and f is the area fraction of the solid surface that contacts water [4, 18]. The Cassie-Baxter model assumes that a water droplet is suspended on rough asperities and allows air trapping between asperities on a surface underneath the droplet, as shown in Fig. 1.

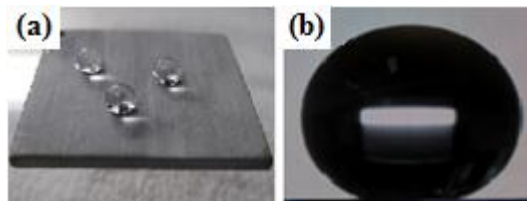


Figure 1: (a) Water droplets on as-prepared superhydrophobic Al surface, (b) water droplet profile on Al surface with $\text{CA} > 150^\circ$.

The XPS signals of C, O and Si, not shown here, of prepared superhydrophobic samples show that the Al samples were well covered with a low surface energy coating of ODTMS. Water droplets easily roll off from coated surface even when the surface is not tilted much (sliding angle of $< 5^\circ$). Based on CA values and applying the Cassie-Baxter equation, a solid fraction (%) area of 11.48 is obtained for the BTSE/ODTMS samples (large amount of air trapped beneath the water droplets). The root-mean-square roughness (R_{rms}), skewness (S_{sk}) and kurtosis (S_{ku}) of coated Al samples were measured using the AFM technique. While the first parameter represents the standard

deviation of surface profile from its mean value, the second parameter (S_{sk}) measures the asymmetry of the profile about its mean plane (being positive for surfaces with peaks and negative for surfaces with valleys), and last parameter (S_{ku}) is a measure of the “spikiness” of the surface [8]. The values of R_{rms} , S_{sk} and S_{ku} were 418 ± 12 , 2.8 ± 0.2 and 12.5 ± 3 , respectively. While the value of R_{rms} measured automatically by AFM was <420 nm, the R_{rms} values measured for the as-received and mirror-polished samples were ~ 109 and ~ 25 nm, respectively. A hydrophobic surface with higher roughness, with more “spiky” peaks, should show improved water repellency and therefore, lower CAH values [8]. The water-solid contact area on this sample was expected to be small, which is consistent with small CAH ($<6^\circ$) and high CA values ($\geq 150^\circ$), characteristic of superhydrophobic surfaces. Also, the high CA and low CAH values observed suggest good surface coverage with ODTMS molecules. Scanning electron micrographs (SEM) images of etched Al sample coated with BTSE/ODTMS at different magnifications are shown in Figure 2, showing rough samples at micro/nanoscales. Both superhydrophobic samples demonstrated good self-cleaning properties as soil mesh was easily carried away by water droplets passing by.

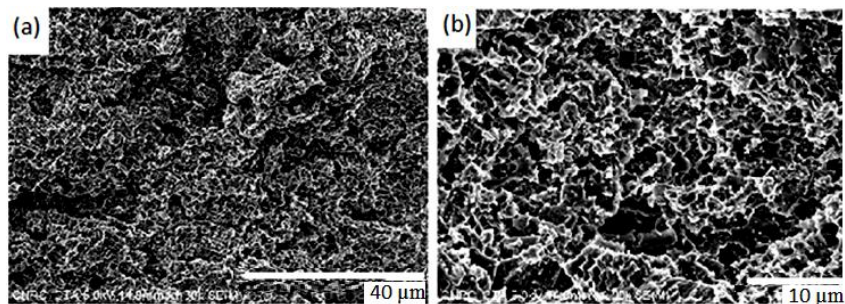


Figure 2: (a and b) Low and high magnification SEM images of 3-min-etched Al sample coated with BTSE/ODTMS.

Figure 3 shows CA and CAH of Al samples coated with BTSE/ODTMS layers as a function of immersion time in nanopure and tap water as well as in basic and acidic solutions. It is obvious that while this sample showed superhydrophobicity, indicating well-coated nano-structured superhydrophobic surfaces, they were found to gradually lose their superhydrophobicity, and completely so after ~ 720 to ~ 1000 -h of immersion in basic and nanopure media, respectively.

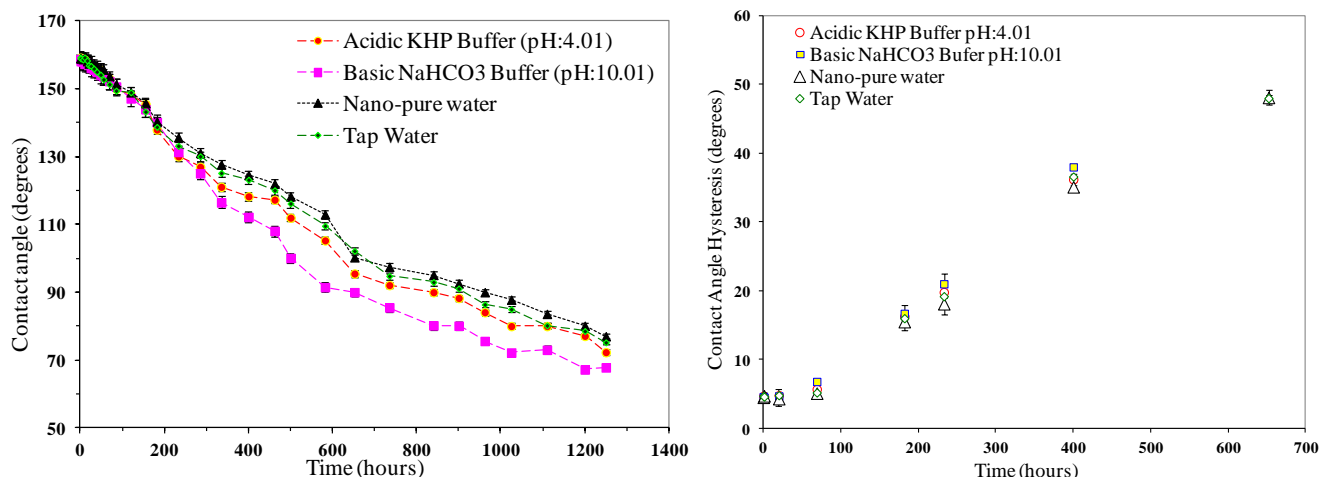


Figure 3: The CA (left) and CAH (right) vs. immersion time for Al coated with BTSE/ODTMS in different conditions.

This is associated with a decrease in CA and an increase in CAH. This tendency to lose surface hydrophobicity is most likely due to the rupture of the Si-O-Si bond between the ODTMS molecules and the BTSE layer caused by hydrolysis of these bonds. By immersing coated Al samples in aggressive media, the ~ 2 -nm ODTMS layer undergoes some degree of degradation initially, as compared to the BTSE layer which is thicker, i.e., ~ 100 nm [19]. Therefore, alkylsilane molecules were removed from the surface, resulting in a decrease in surface superhydrophobicity. The top layer was not believed to be dense enough to prevent water molecules from penetrating through the coating and reaching the coating-substrate interface. This caused hydrolysis of the Si-O-Si bond, through which the ODTMS molecules were attached to the surface. However, the BTSE underlayer created a dense coating on Al surface to prevent corrosion acceleration, e.g. water going through underlayer coating and reaching the underneath metallic substrate.

B. Ice-repellent performance

Since dynamic hydrophobicity may play an important role in ice repellency, more specially for nanostructured substrates, glaze ice was prepared in a wind tunnel at subzero temperature ($-10\text{ }^{\circ}\text{C}$) by spraying water micro-droplets with an average size of $\sim 65\mu\text{m}$ to simulate outdoor icing condition [3-10, 16]. The procedure to evaluate ice adhesion strength was previously reported in detail elsewhere [3-10, 16]. Figure 4 shows the shear stress of ice detachment as a function of icing/de-icing cycles on coated Al samples. For each coating studied, one sample was subjected to 12 successive de-icing tests. Due to high mobility of water (low CAH), the ice accretion process was delayed on these surfaces. Both ODTMS and BTSE/ODTMS samples showed close values of shear stress, with very similar ice adhesion strength (IAS) on alkyl-grafted samples.

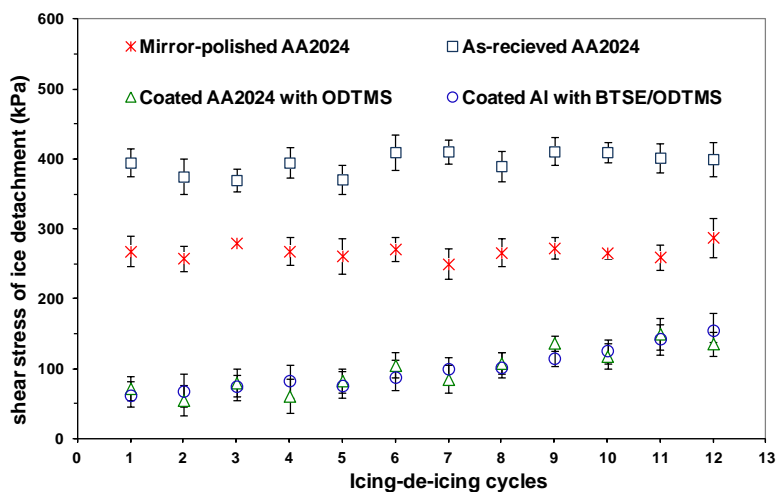


Figure 4: Shear stress of ice detachment vs. icing/de-icing cycle for Al surface coated with ODTMS and BTSE/ODTMS.

While as-received and mirror-polished Al was used as standard reference showing initial values of shear stress of ice detachment of $\sim 370\pm 30\text{ kPa}$ and $\sim 270\pm 20\text{ kPa}$, respectively, its coated counterparts with ODTMS or BTSE/ODTMS coatings showed reduced values of $\sim 62\text{ kPa}$ which is ~ 6 times lower than those on as-received Al standard (low CAH). This reduction is attributed to the presence of micro-/nano-hierarchical surface structures and low surface energy layers. However, superhydrophobic samples demonstrated increase of ice adhesion strength if compared to the as-prepared surfaces. The observed increase in ice adhesion strength is believed to be associated with both a decay of the ODTMS layer and of a larger ice-solid contact area, after 12 icing/de-icing cycles [5]. Meanwhile, water repellency of the coated sample gradually decreased over repeated icing/de-icing cycles (CA decreased and CAH increased). The top layer degraded on the BTSE underlayer in a manner similar to what happened on Al surfaces. Water molecules can attack the R-Si-O- bond to hydrolyze it, resulting in hydrophilic $-\text{OH}$ groups on the surface.

C. Anti-corrosive performance of double layer superhydrophobic coating

Aluminium alloy 2024 is an alloy with Cu as major element and thus, with poor corrosion resistance. Therefore, developing anti-icing coatings on Al substrates highlights the necessity of improving their anticorrosive resistance. The potentiodynamic polarization curves of (a) bare AA2024 and the superhydrophobic coatings of (b) ODTMS and (c) BTSE/ODTMS on the Al alloy in 3.5 wt.% NaCl solution are presented in Fig. 5. The E_{corr} and j_{corr} values derived from corresponding polarization curves, using *Tafel* extrapolation, are summarized in Table 2. It is evident in Fig. 5 and Table 2 that the value of E_{corr} positively increases from $-0.71\pm 0.03\text{ V}$ for bare Al to $-0.62\pm 0.02\text{ V}$ and $-0.53\pm 0.02\text{ V}$ for the superhydrophobic coatings of ODTMS and BTSE/ODTMS, respectively.

Table 2: Potentiodynamic results of bare and coated AA2024 with ODTMS and BTSE/ODTMS in 3.5 wt.% NaCl solution.

| Sample | E_{corr} (V vs. SCE) | j_{corr} (μAcm^{-2}) |
|--------------------|----------------------------------|---|
| Bare AA2024 | -0.71 ± 0.03 | 24.4 |
| ODTMS Coating | -0.62 ± 0.02 | 1.12 |
| BTSE/ODTMS Coating | -0.53 ± 0.02 | 0.008 |

The positive shift observed in E_{corr} is obviously due to the improvement of the protective performance of the superhydrophobic coating formed on the AA2024 substrate. In the meantime, the corrosion current density, j_{corr} , of the superhydrophobic coating of BTSE/ODTMS ($8.04\text{E-}9 \text{ Acm}^{-2}$) had a decrease of about 4 orders of magnitude as compared to that of bare ($2.44\text{E-}5 \text{ Acm}^{-2}$) and a decrease of 3 orders of magnitude as compared to ODTMS ($1.12\text{E-}6 \text{ Acm}^{-2}$). These results indicate that the double-layered superhydrophobic coating of BTSE/ODTMS improved corrosion resistance of Al surfaces as compared to bare Al on which the Al oxide layer is permeable to moisture and is prone to undergo dissolution in humid environment (accelerated corrosion). Therefore, the barrier property of the BTSE/ODTMS-modified Al sample was improved significantly as compared to an unmodified sample or even to an Al surface coated with ODTMS (single layer).

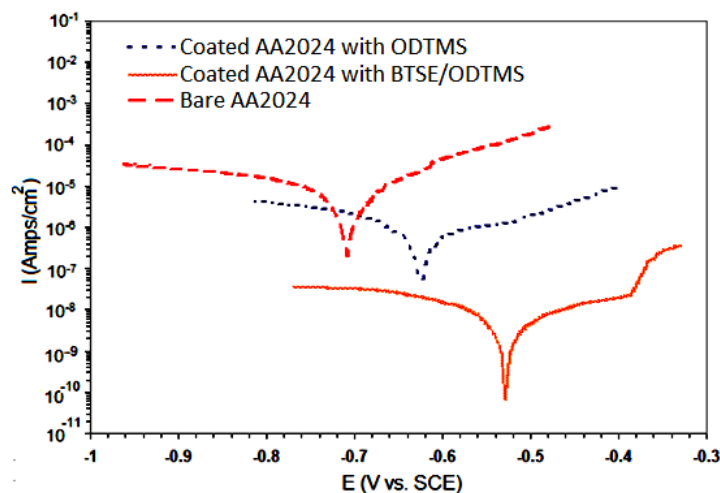


Figure 5: Polarization curves of AA2024 with and without coating.

The anti-corrosive properties of coated and bare samples were further studied by cyclic corrosion test. These samples were exposed alternatively to salt mist, dry and wet conditions in accordance with ISO14993 [17], following 3 repeating step: 2-hr exposure to a continuous indirect spray of neutral (pH: 6.5-7.2) salt water solution at a rate of $2\text{ml-}80\text{cm}^{-2}/\text{hour}$ at $35\text{ }^{\circ}\text{C}$, then, 4 hrs of air drying in a climate of $>30\% \text{ RH}$ at $60\text{ }^{\circ}\text{C}$ and finally a 2-hr exposure to a wetting (95 to $100\% \text{ RH}$) at $50\text{ }^{\circ}\text{C}$. The bare Al samples exhibited extensive corrosion after only 8 cyclic corrosion cycles with appearance of numerous black dots (pits) in micrometer scale. Meanwhile, the size and density of the black dots increased as the number of salt spray cycles increased, which was due to increasing localized corrosion expansion.

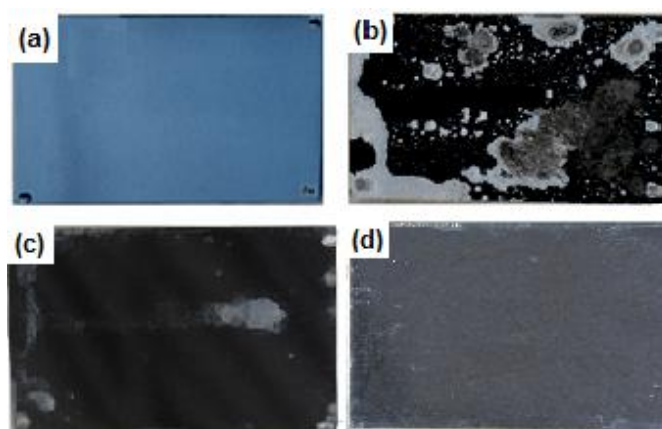


Figure 6: Optical images of bare AA2024 before (a) and after (b) an 18-cycle corrosion test for ODTMS coated AA2024 alloy (c) and for BTSE/TMSOD coated alloy (d) after test.

However, the earlier stage of corrosion was observed after 18 cycles of exposure in the case of samples coated with ODTMS. Small traces of corrosion were observed in the case of the Al sample coated with BTSE/ODTMS, even after 81 cycles of exposure (Fig.6). These observations confirm the results presented earlier in Fig. 5 by the potentiodynamic polarization curves showing the corrosion resistance improvement of samples modified with BTSE layers (less defect areas and dense enough) compared to bare or sample coated with ODTMS.

IV. CONCLUSIONS

In this study, alkyl-terminated nano-structured superhydrophobic surfaces were prepared by depositing a layer of ODTMS on BTSE-grafted AA2024 or rough AA2024 substrate. Both samples demonstrated excellent superhydrophobic and self-cleaning properties. Their durability in different conditions was tested by means of CA measurements, demonstrating gradual loss of hydrophobicity after ~720 to ~1000-h of immersion in basic and nanopure media, respectively, associated with a decrease of water CA. Ice-releasing properties of the coated surfaces were investigated by accumulating glaze ice in a wind tunnel at subzero temperature. While bare Al showed average ice detachment shear stress of $\sim 370 \pm 30$ kPa, its counterparts coated with ODTMS or BTSE/ODTMS showed reduced values of ~ 62 kPa which is ~ 6 times lower than those of the as-received Al standard (low CAH). This reduction is attributed to the presence of micro-/nano-hierarchical surface structures and low surface energy layers. These values gradually increased after as many as 12 successive icing/de-icing cycles. The increase in ice adhesion strength is believed to be associated with both a decay of the ODTMS layer and a larger ice-solid contact area after 12 icing/de-icing cycles. The electrochemical measurement results demonstrated that corrosion potential of the BTSE/ODTMS coating increased significantly, and its corrosion current density decreased by 4 orders of magnitude as compared to those on bare samples. These results showed that the BTSE underlayer on the AA2024 substrate provides particularly enhanced corrosion resistance which would be an excellent approach to improving anti-corrosive performance of metallic surfaces for outdoor applications instead of the toxic chromate-based coatings currently in use.

ACKNOWLEDGEMENTS

This research work has been conducted within the framework of the NSERC/Hydro-Quebec/UQAC Industrial Chair on Atmospheric Icing of Power Network Equipment (CIGELE) and the Canada Research Chair on Atmospheric Icing Engineering of Power Networks (INGIVRE) at Université du Québec à Chicoutimi. The authors would like to thank the CIGELE partners (Hydro-Québec, Hydro One, Réseau Transport d'Électricité (RTE), Rio Tinto Alcan, General Cable, K-Line Insulators, Dual-ADE, and FUQAC) whose financial support made this research possible.

REFERENCES

- [1] M. Farzaneh, "Atmospheric Icing of Power Networks", Ed., Springer, Berlin, pp. 320, August 2008.
- [2] H. Saito, K. Takai, G. Yamauchi, "Water- and ice-repellent coatings". *Surface Coatings International*, vol. 80, pp. 168, 1997.
- [3] S. A. Kulinich, M. Farzaneh, "Hydrophobic properties of surfaces coated with fluoroalkylsiloxane and alkylsiloxane monolayers", *Surface Science* vol. 573, pp. 379, 2004.
- [4] S. Farhadi, M. Farzaneh, S. Simard, "Nanostructured ultra superhydrophobic Al surfaces: stability and icephobic properties", *International Journal of Theoretical and Applied Nanotechnology*, vol. 1, pp. 38, 2013.
- [5] S. A. Kulinich, M. Farzaneh, "How wetting hysteresis influences ice adhesion strength on superhydrophobic surfaces", *Langmuir*, vol. 25, pp. 8854, 2009.
- [6] S. Farhadi, M. Farzaneh, S. A. Kulinich, "Anti-Icing Performance of Superhydrophobic Surfaces", *Applied Surface Science*, vol. 257, pp. 6264, 2011.
- [7] Z. Ghalmi, R. Menini, M. Farzaneh, "Effect of different aluminium surface treatments on ice adhesion strength", *Advanced Materials Research*, vol. 409, pp. 788, 2012.
- [8] F. Arianpour, M. Farzaneh, S. Kulinich, "Hydrophobic and ice-retarding properties of doped silicone rubber coatings", *Applied Surface Science*, vol. 265, pp. 546, 2013.
- [9] F. Arianpour, M. Farzaneh and S. A. Kulinich, "Nanopowder-Doped Silicone Rubber Coatings for Anti-Ice Applications", *Scanning Electron Microscopy*, 497, 4, 2010.
- [10] S. Farhadi, M. Farzaneh and S. Simard "On Stability and Ice-Releasing Performance of Nanostructured Fluoro-Alkylsilane-Based Superhydrophobic AA2024 Surfaces", *Inter. J. Theor. and Appl. Nanotechnology*, 2012.
- [11] Z. Guo, F. Zhou, J. Hao, W. Liu, "Stable Biomimetic super-hydrophobic engineering materials", *Journal of the American Chemical Society*, vol. 127, pp.15670, 2005.
- [12] Y. Shaojun, S. O. Pehkonenb, L. Bin, Y. P. Ting, K.G. Neoh, E. T. Kang, "Superhydrophobic fluoropolymer-modified copper surface via surface graft polymerisation for corrosion protection", *Corrosion Science*, vol. 53, pp. 2738, 2011
- [13] V. F. Petrenko and S. Peng, "Reduction of ice adhesion to metal by using self-assembling monolayers (SAMs)", *Can. J. Phys.*, vol. 8, pp. 387-393, 2003.
- [14] M. Farzaneh, "Systems for prediction and monitoring of ice shedding, anti-icing and de-icing for overhead lines", CIGRÉ WG B2.29, CIGRE Publications, Technical Brochure #438, pp. 100, 2010.
- [15] E. H. Andrews, H. A. Majid, N. A. Lockington, "Adhesion of ice to a flexible substrate", *Journal Materials Science*, vol. 19, pp. 73, 19984.
- [16] V. K. Croutch and R. A. Hartley, "Adhesion of ice to coatings and the performance of ice release coatings", *J. Coat. Technol.*, vol. 64, pp. 41, 1992.
- [17] <http://www.matweb.com/search/DataSheet.aspx?MatGUID=57483b4d782940faaf12964a1821fb61>.
- [18] L. Thomsen, B. Watts, D. Cotton, J. Quinton and P. Dastoor, *Surf. Interface Anal.*, 37, 472, 2005.
- [19] X. Yao, Q. W. Chen, L. Xu, Q. K. Li, Y. L. Song, X. F. Gao, D. Quere and L. Jiang, *Adv. Funct. Mater.*, 20, 656, 2010.
- [20] S. Farhadi, M. Farzaneh and S. A. Kulinich, "Preventing Corrosion and Ice Accretion on Aluminium Surfaces Applying Organic and Inorganic Thin Films", MSc thesis, UQAC, Dec. 2010.
- [21] http://www.iso.org/iso/home/store/catalogue_tc/catalogue_detail.htm?csnumber=24372.
- [22] ATLAS Weathering Testing Guidebook.
- [23] A. Franquet, C. Le Pen, H. Terryn, et al., "Effect of bath concentration and curing time on the structure of nonfunctional thin organosilane layers on aluminium", *Electrochim. Acta*, vol. 48, pp. 1245, 2003.